Chinese J. Chem. Eng., **13** (3) 297 – 302 (2005)

Numerical Simulation of the Scalar Mixing Characteristics in Three-dimensional Microchannels*

LIU Yanhua(刘演华), LIN Jianzhong(林建忠) and BAO Fubing(包福兵)**
Department of Mechanics, State Key Laboratory of Fluid Power Transmission and Control, Zhejiang University, Hangzhou 310027, China

SHI Xing(石兴)
Department of Mechanical Engineering, National University of Singapore, Singapore, 119260

Abstract Based on the transport phenomena theory, the passive mixing of water and ethanol in different three-dimensional microchannels is simulated numerically. The average variance of water volume fraction is used to index the mixing efficiency in the cases with different Reynolds number and different fabricated mixers. The results show that the efficiency of liquid mixing is progressively dependent on the convective transport as the Reynolds number increases. The efficiency of serpentine microchannel decreases with the increasing Reynolds number in the laminar regime. Altering the aspect ratio of channel inlet section has no significant effect on the mixing efficiency. Increasing the area of channel inlet section will cause the decrease of the mixing efficiency. The mixing in serpentine channels is the most efficient among three different mixers because of the existence of second flow introduced by its special structure.

Keywords microchannel, mixer, mixing efficiency, numerical simulation

1 INTRODUCTION

It is impressively felt that the mechanisms of flow and heat or mass transfer in microchannels are still not understood clearly. For instance, the viscous dissipation effect is too significant to be neglected due to the high velocity gradient as the flow dimension approaches the micro-level[1]. Electroosmosis is one of the most important means to drive the channel flow. Different material has different electric potential introduced by the wall and will have quite different effect on the flow medium[2]. Further more, pure liquids behave quite differently from the electrolytic solution[3]. In all of the above situations, there is a basic problem: mixing, which bears significant relevance in microfabricated systems for complex chemical synthesis. Investigating different method for mixer fabrication and their mixing efficiency will have great experimental and practical meaning. For the gas, the mixing will be completed in very short time and small spatial volume, while it may be especially inefficient for the solutions containing macromolecules[4]. In the mixer with micro-dimensions, the flow is laminar and no flow turbulence is present to promote the rapid mixing. Therefore, some other mechanism must be introduced to enhance mixing.

Passive mixer has been widely used because it is relatively simple to fabricate and implement. Gobby *et al.*[5] and Andrew *et al.*[6] utilized the same methods to study the mixing characteristics of T-type microfluidic mixers, in which Gobby *et al.* employed oxygen and methanol as the media to study the mixing. The result shows that there exist some structure characteristics and factors that influence the mixing efficiency. Chainarong *et al.*[7] investigated the mixing characteristics of a square-wave channel by introducing the electromagnetic force into the mixing. Liu *et al.*[8] studied experimentally the mixing characteristic of passive serpentine mixers with the method of determining the color intensity of the mixture from phenolphthalein and sodium hydroxid solutions. The results showed that the mixing ability of serpentine channels is stronger than that of other two mixers and the mixing efficiency is enhanced as the Reynolds number increases.

In spite of the well-documented theoretical evidence for the passive mixer, the effect of mixer cross-sectional shape on the mixing and the description of mixing efficiency quantitatively are still not well understood and are subjected to debate. Therefore, the present paper aims at giving the mixing efficiency quantitatively by numerical simulation, and provides the information about the effect of serpentine mixer cross-section (rectangle, $y \times z$ = 150 μm×300 μm, 300 μm×150 μm, 400 μm×200 μm) on the mixing characteristics. Main attention is paid to the serpentine channel mixer.

2 SERPENTINE MIXER GEOMETRY

This paper investigates the characteristic of three types of mixers (serpentine, square-wave, straight) nu-

Received 2004-08-05, accepted 2004-12-26.
* Supported by the National Natural Science Foundation of China (No. 20299030).
** To whom correspondence should be addressed. E-mail:mecjzlin@public.zju.edu.cn

merically. A schematic of three mixers' geometry is shown in Fig. 1. The basic building block of serpentine mixer (top) is a "C-shaped" section that turns the fluid through 180° hand lies in a plane. The channel guides the fluid through an in-plane "C-shaped" section, rotates the fluid by 90°, and then guides the fluid through another in-plane C-shaped section. 20 sections are used in the simulation. A "square-wave" channel (middle), similar to "zig-zag" channel and a straight channel (bottom) are also fabricated as shown in Fig. 1. The square-wave has 24 "C-shaped" sections lying in the same plane and the straight channel's length is 22 mm. All the outlets are joined with a 900 μm long channel while the inlets are joined with a T-junction. The origin of the coordinate is at the union of T-junction with the channels. Two separate fluid streams, *e.g.*, water and ethanol, flow into channel through the T-junction. The inlet cross section is 300 μm×150 μm. The aspect ratio is defined as $z/y = 150/300 = 1/2$.

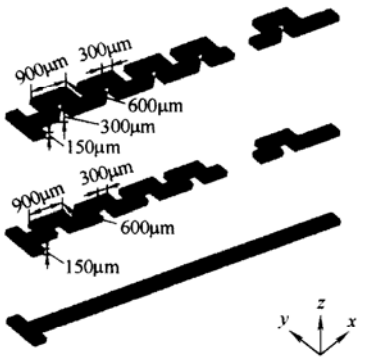

Figure 1 Schematic of three types of mixers

3 THEORETICAL MODEL

3.1 Mathematical model

The equations governing the flow are continuity equation, Navier-Stokes momentum equation and species convection-diffusion equation[10] as listed below:

$$\begin{aligned} &\nabla \cdot \boldsymbol{v} = 0 \\ &\frac{D\boldsymbol{v}}{Dt} = -\frac{1}{\rho}\nabla p + \upsilon \nabla^2 \boldsymbol{v} \\ &\frac{D\chi_a}{Dt} = D_{ab}\nabla^2 \chi_a \end{aligned} \tag{1}$$

In order to get the dimensionless forms of Eq. (1), we define

$$\boldsymbol{v}^* = \boldsymbol{v}/U_0, x^* = x/D_c, p^* = p/\rho U_0^2, t^* = U_0 t/D_c,$$
$$\chi_a^* = \chi_a/\chi_0$$

where $U_0 = Q/S$ (Q is the volume flux and S is the cross section area), U_0, D_c, ρ and χ_0 stand for average velocity in the serpentine channel, characteristic dimension of the channel, density of water and the initial mass fraction respectively. Generally, D_{ab} has a magnitude of 10^{-9} for liquids.

Using the definition above, the dimensionless forms can be rewritten as

$$\begin{aligned} &\nabla^* \cdot \boldsymbol{v}^* = 0 \\ &\frac{D\boldsymbol{v}^*}{Dt^*} = -\nabla^* p^* + \frac{1}{Re}\nabla^{*2} v^* \\ &\frac{D\chi_a^*}{Dt^*} = \frac{1}{ReSc}\nabla^{*2}\chi_a^* \end{aligned} \tag{2}$$

For this specified case, the boundary condition should be described as follows.

$$\begin{cases} \boldsymbol{v}^*|_{\text{wall}} = 0 \\ \boldsymbol{v}^*_{\text{water}}|_{\text{in}} = \boldsymbol{v}^*_{\text{ethonal}}|_{\text{in}} = 1 \\ \boldsymbol{v}^*|_{\text{out}} = \boldsymbol{v}^*|_{\text{out}-1} \end{cases}$$

$$\begin{cases} \chi_a^* = 1 \quad \text{(water inlet)} \\ \chi_a^* = 0 \quad \text{(ethanol inlet)} \\ J_{\text{wall}} = 0 \\ \chi_a^*|_{\text{out}} = \chi_a^*|_{\text{out}-1} \end{cases} \tag{3}$$

where J is the flux of the mass, out—1 means the inside layer adjacent to the outlet boundary.
Reynolds number is defined as

$$Re = \frac{\rho U_0 D_c}{\mu} \tag{4}$$

and Schmidt number is

$$Sc = \frac{\mu}{\rho D_{ab}} \tag{5}$$

Derivations and details of the species convection-diffusion equation can be found in Bird *et al.*[10]. The left hand side of the equation is the material derivative of the mass fraction and right hand side of the equation is the diffusion term in terms of the mass fraction. From the equation, we know that the change of the mass fraction can be attributed to two parts: convection and diffusion. If the reaction is introduced into the system, an additional source term may be included at the right hand side and the equation may be called reaction-diffusion equation which can be found in many situations with combustion or chemical process[3]. In the range of microchannels considered here, the macroscopic hydrodynamic principles still apply.

The product of Schmidt number (Sc) and Reynolds number (Re), termed Peclet number (Pe), describes the ratio of mass transport by convection to that by diffusion. The convection dominates the transfer process when $Pe > 2$, and in this paper, the condition of $Pe \gg 2$ prevails. In order to present the channel geometry, a characteristic dimension is defined as

$$D_c = \frac{2hw}{h+w} = 0.2\,\text{mm} \tag{6}$$

where, h and w represent the height and the width of the cross section, respectively. The Knudsen number $Kn \ll 0.001$, so the slip effect of boundary can be omitted. The diffusion coefficient D_{ab} in water and ethanol at 25 ℃ is $1.03 \times 10^{-9}\ m^2 \cdot s^{-1}$[14]. All calculated cases are in laminar flow regime.

Equation (2) is solved numerically using FLUENT for flow field and FORTRAN 90 complier and TECPLOT9.0 for post-processing. The hardware configuration is 2.8 GHz CPU, 1 G memory and 64 M display card. In the computation, the time-independent instance is considered, and the SIMPLEC method is implemented to couple the pressure and velocity while all spatial discretizations are performed using the second order UPWIND method. The whole region in the serpentine is discretized with hexahedral cell and coupled with a domain decomposed and matched method. There are 1 161 000 cells and 1 270 876 nodes in all.

3.2 Parameter describing the mixing

The x direction is assumed the mainstream direction and several planes running parallel to y-z plane are picked out and analyzed. In order to describe the extent of mixing quantitatively, the volume fraction's average variance in each y-z plane is defined as

$$\sigma = \sqrt{\frac{1}{n}\sum_{1}^{n}(\varpi - 0.5)^2} \tag{7}$$

An index similar to that used by Liu *et al.*[9] in studying the oil-water two-phase flow in the horizontal pipes experimentally. Here, ϖ represents the volume fraction of species. 0.5 means the ideal status that the mixture has been completely blended homogeneously. n denotes the maximum number of the nodes discretized on the specified plane. According to the definition of Eq. (7), σ can be used to describe the extent departed from the ideal status ($\varpi = 0.5$). When species stream flows pass through a same distance along the stream direction, sufficient mixing gets a smaller σ and inefficient mixing leads to a larger σ, *i.e.*, the smaller the average variance σ is, the higher the mixing efficiency is. In this paper, six kinds of flow situations listed in Table 1 are calculated and compared, where, v_{in} is velocity at the inlet of the T-junction.

Table 1 Six flow situations simulated

Re	v_{in}, $m \cdot s^{-1}$
0.4	0.00103
1	0.0027875
4	0.0103
10	0.02575
25	0.064375
70	0.18025

4 RESULTS AND DISCUSSION

4.1 The effect of *Re* on the mixing efficiency

Figure 2 depicts the relationship between average variance of volume fraction along the centreline distance L from origin to a definite y-z plane in the channel with different Re. It can be seen that, for a definite L, lower Re leads to a smaller average variance which means a higher mixing efficiency. Such difference results are because a lower Reynolds number corresponds a sufficiently long contacting time, and the mixing (mostly convection) plays a major role. When the Reynolds number increases, the mixing time gets shorter and the mixing can not be completed more efficiently in a shorter time.

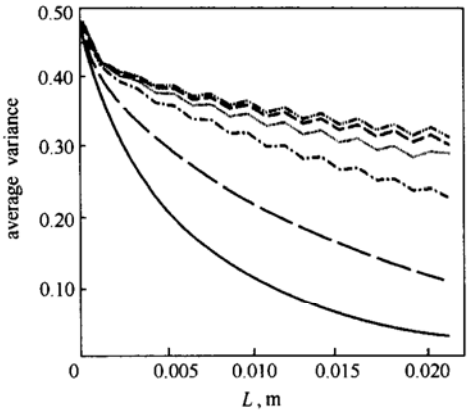

Figure 2 Relationship between the mixing efficiency and flow distance for different *Re*
Re: —— 0.4; − − − 1; − · − 4; ····· 10; - - - - 25; − ··· − 70

In Fig. 2, when Re is greater than 1, the curves exhibit distinct fluctuation while tending to drop with L. This may attribute to the secondary flow and chaotic mixing. The fabrication of serpentine channel makes the flow complicated and the particle path chaotic. The fluctuation period equals to that of the serpentine geometry appearing in the channel. At the two side of the "C-shaped" sections, the flow pattern is reversed. This contributes to the fluctuation phenomena as shown in Fig. 2. Because the sampling plans are all in the middle of each "C-shaped" sections, the curve exhibits peak and valley alternately. At the latter of this paper, we can see that the square-wave channel also has the similar phenomena but is not obvious, and the straight channel has almost none.

Figure 3 represents the curve of the average variance of water with Reynolds number changing after a same length $L = 21$ mm. L is the centerline length along the channel. The curve is fitted by the second spline function. We can see that the average variance is linear with Reynolds number when Re is lower ($\leqslant 4$) and changes inconspicuously when Re is larger than a certain number. The result shows that the

mixing is determined by both convection and the contacting time. Long contacting time suggests that it has enough time to complete the mixing by diffusion only. When Re number is less than the order of 1, the intensity of convection affects the mixing efficiency is almost the same irrespective of the contacting time. When Re has the magnitude of 10, the convection is enhanced while the mixing time decreases. The combining effect makes the mixing efficiency almost the same on the macroscale. It can be concluded that if Reynolds number continues to increase, the convective influence becomes stronger and dominants the mixing comparing with the mixing time. The calculating results show that the mixing efficiency is higher in the case of $Re = 900$ than the case of $Re = 70$ (the flow is still laminar when $Re = 900$).

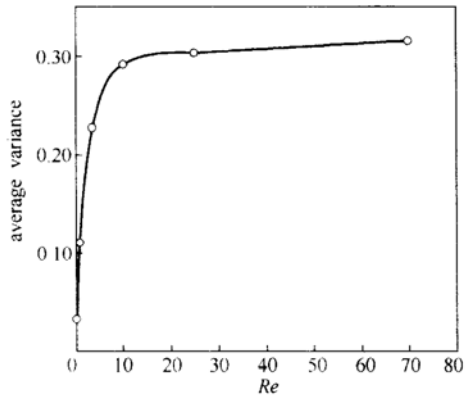

Figure 3 Mixing efficiency for different Re at $L = 21$ mm

4.2 The effect of inlet cross section on the mixing efficiency

Rotating the T-type junction for 90 degree around the x axis, the inlet cross section becomes 150 μm×300 μm and the aspect ratio becomes 4 times of the former case (Case 1). This case is denoted as Case 2. The inlet cross section is changed to 400 μm×200 μm and the aspect ratio remains original (Case 3). The volume fraction average variances are calculated for Cases 1, 2 and 3 at $Re = 0.4$, 1 and 70, respectively and the results are shown in Figs. 4 and 5.

From Figs. 4 and 5, it can be concluded that the variation of the aspect ratio with the same cross section area can not efficiently change the mixing efficiency. When the aspect ratio is kept the same, the channel having larger cross section has lower mixing efficiency compared with Case 1. Although high aspect ratio means that the contacting area of two liquids becomes large, the mixing efficiency becomes lower than Case 1 at the contrary. It illustrated that the mixing for liquid is much different from that for gas due to the different diffusion coefficient. The dispersion of liquid is less dependent on the molecular diffusion but more on the convection. It is consistent with the illustration that the convective effect dominants the mixing when Pe is greater than 2. Again, keeping the aspect ratio constant and changing the cross section area of inlet will have no action to improve the mixing efficiency. Large cross section area means that it will take more time to reach the equilibrium at the near wall. Hence, the average variance of Case 3 for $Re = 0.4$ is even higher than that of Case 1 with $Re = 1$.

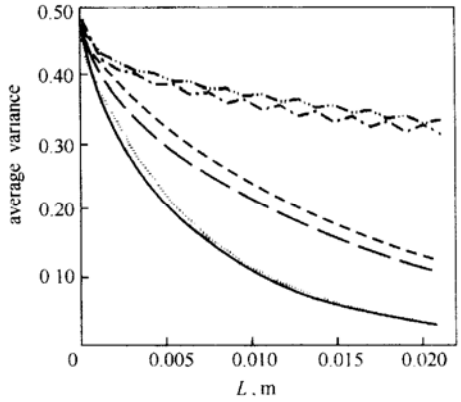

Figure 4 The mixing efficiency for Cases 1 and 2
Case 1: —— $Re = 0.4$; – – – $Re = 1$, – · – $Re = 70$;
Case 2: ····· $Re = 0.4$; - - - - $Re = 1$; – · – $Re = 70$

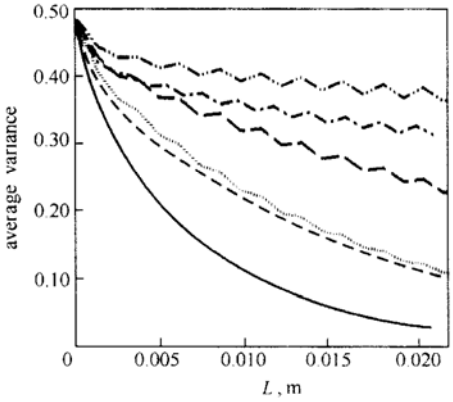

Figure 5 The mixing efficiency for Cases 1 and 3
Case 1: —— $Re = 0.4$; - - - - $Re = 1$; – · – $Re = 70$;
Case 3: ····· $Re = 0.4$; – – – $Re = 1$; – ·– $Re = 70$

4.3 The effect of mixer type on the mixing efficiency

Figures 6—9 show the volume fraction average variances for three different types of channels. The definition of L for three types of mixers is the same. In spite of different Re, the mixing efficiency of serpentine channel is the highest among the three. When $Re = 0.4$, for instance, the other two channels need to run twice distance of the serpentine at least according to curve fitting. It can also be found directly that the efficiency curves of square-wave channel and serpentine channel have the tendency of approaching with each other and being away from the straight channel. All curves of average variance rise when Re increases,

which means the mixing efficiency falls down. But the falling speed for the case of serpentine channel and square-wave channel is not so rapid as the case of the straight channel. This phenomenon attributes to the secondary flow as shown in Fig. 10.

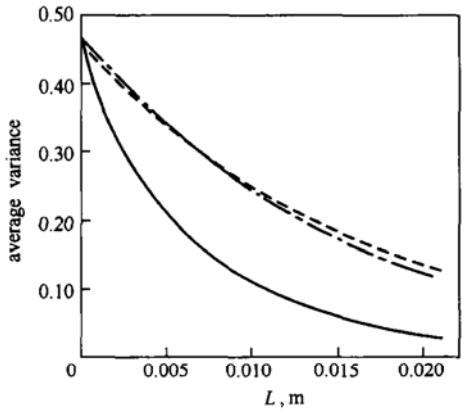

Figure 6 The mixing efficiency for three mixers at $Re = 0.4$

—— serpentine; – – – square-wave; – · – strainght

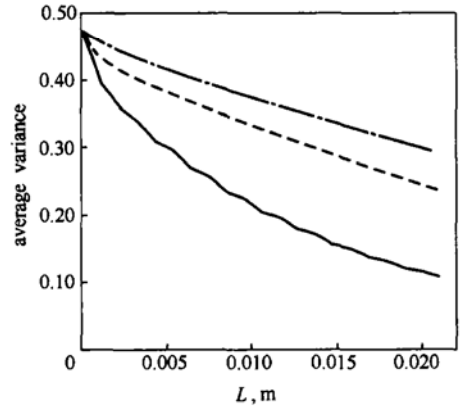

Figure 7 The mixing efficiency for three mixers at $Re = 1$

—— serpentine; – – – square-wave; – · – strainght

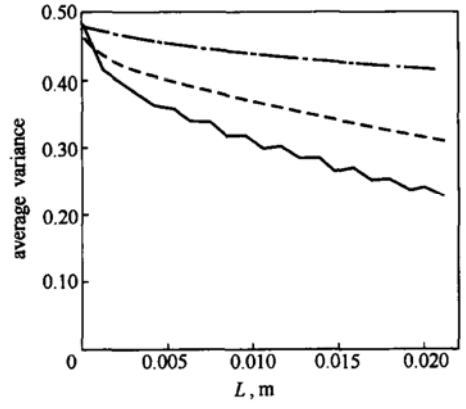

Figure 8 The mixing efficiency for three mixers at $Re = 4$

—— serpentine; – – – square-wave; – · – strainght

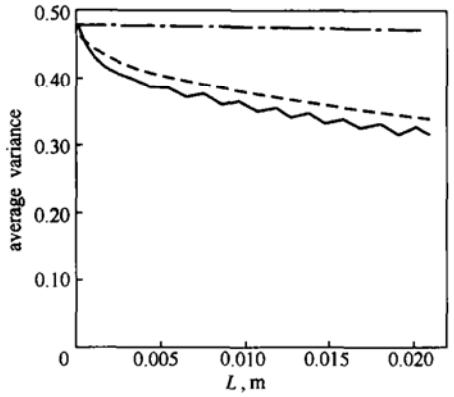

Figure 9 The mixing efficiency for three mixers at $Re = 70$

—— serpentine; – – – square-wave; – · – strainght

Figure 10 is obtained by the post processing software "Tecplot9.0" and it shows the volume fraction contour and stream lines at the sections of $x = 4$ mm (in the 7th "C-shape") and $y = 0$ mm. (in the 6th "C-shape") respectively. Figs.10 (a) and (c) are figures of volume fraction contour for water ($Re = 1.0$) and the figures appear distinct dissymmetry. Figs. 10 (b) and (d) are the figures of stream line ($Re = 25$), in which the obvious vortices can be seen. Because of the secondary flow aroused by the structure, the mixing is enhanced in the serpentine channel. The secondary flow is also observed in the square-wave channel while the Re is over certain value but cannot be found in straight channel. As a result, the mixing efficiency of serpentine channel and square-wave channel is much higher than that of straight channel. It offers us a guideline to designing a mixer with high efficiency, *i.e.*, enhancing the secondary flow to speed up the mixing as much as possible.

5 CONCLUSIONS

From the analysis above, the following conclusions can be derived.

(1) For the cases with two input liquids, the mixing efficiency decreases with Reynolds number when Reynolds number is less than 900.

(2) The mixing efficiency is related to the mixing time and the flow convective intensity. The mixing is decided by diffusion at first, and is dominated by convective effect more obviously as Re increases.

(3) For serpentine channel, the case with small aspect ratio of inlet cross section has a little higher efficiency, but the variation of aspect ratio has no distinct effect on the mixing efficiency. Large inlet cross-section area makes the efficiency low instead.

(4) With the same length of centerline, the mixing efficiency in the serpentine channel is obvious higher than that in the square-wave and straight channels because of a distinct secondary flow in the serpentine channel.

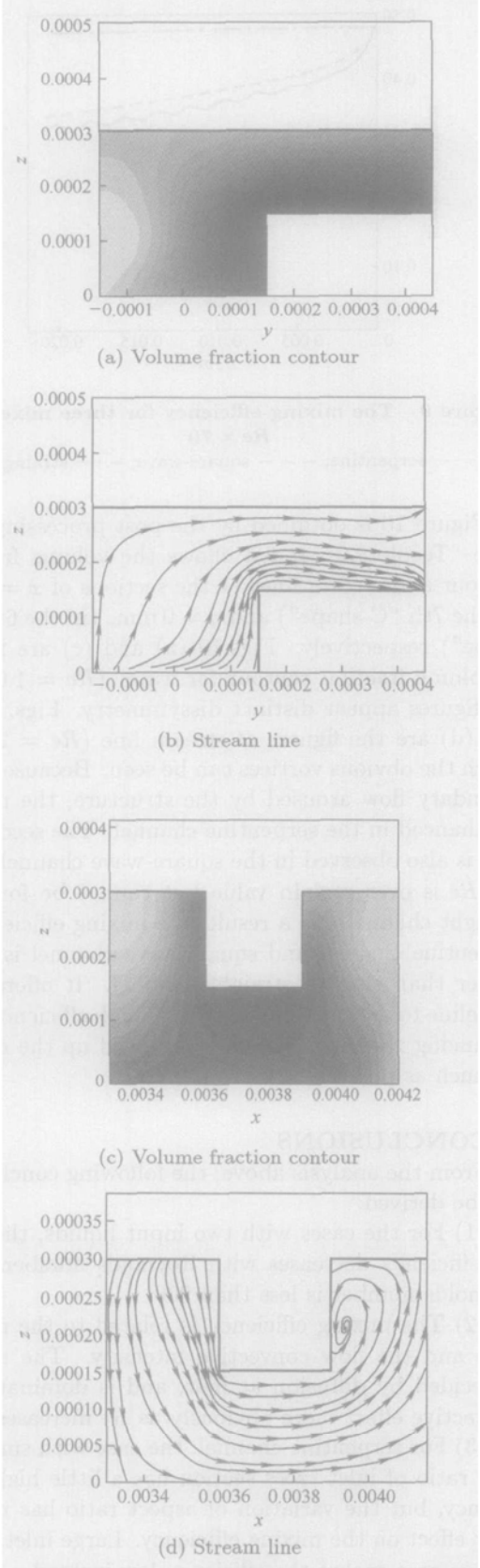

Figure 10 The information of flow and diffusion at a section with $Re = 1$ and $Re = 25$

NOMENCLATURE

D_{ab}	diffusion coefficient between a and b, $m^2 \cdot s^{-1}$
D_c	hydraulic diameter, mm
h	height of cross section of channel, mm
J	flux of mass
L	distance along the centerline, m
p	pressure, Pa
Q	volume flux, $m^3 \cdot s^{-1}$
t	time, s
S	cross-section area, m^2
U_0	inlet velocity of the channel, $m \cdot s^{-1}$
v_{in}	inlet velocity of the T-type mixer, $m \cdot s^{-1}$
v	velocity vector
w	width of cross-section, mm
σ	average variance of volume fraction
χ_a	mass fraction of species a
ϖ	volume fraction of species
Kn	Knudsen number
Pe	Peclet number
Re	Reynolds number ($Re = 0.4/1/4/10/25/70$)
Sc	Schmidt number

Superscripts

*	dimensionless form

REFERENCES

1 Xu, B., Ooi, K.T., Mavriplis, C., Zaghloul, M.E., "Viscous dissipation effects in microtubes and microchannels", *In. J. Heat Mass Transfer*, **47**, 3159—3169 (2004).
2 Yang, R-J., Fu, L.-M., Lin, Y-C., "Electroosmotic flow in microchannels", *J. Colloid Interf. Sci.*, **239**, 98—105 (2001).
3 Ye, C.Z., Li, D.Q., "3-D transient electrophoretic motion of a spherical particle in a T-shaped rectangular microchannel", *J. Colloid Interf. Sci.*, **272**, 480—488 (2004).
4 Brody, J.B., Yager, P., "Low Reynolds number micro-fluidic devices", In: Proc. Solid-State Sens. Actuator Workshop, Hilton Head, SC, 105—108 (1996).
5 Gobby, D., Angeli, P., Gavriilidis, A., "Mixing characteristics of T-type microfluidic mixers", *J. Micromech. Microeng.*, **11**, 126—132 (2001).
6 Andrew, E.K., Yager, P., "Theoretical analysis of molecular diffusion in pressure-driven laminar flow in microfluidic channels", *Biophy. J.*, **80**, 155—160 (2001).
7 Chainarong, C., Koji, F.N.K., "Mixing enhancement in a micro serpentine conduit for cell Sorting", In: 5th International Conference on Multiphase Flow, Paper No. 405, Yokohama (2004).
8 Liu, R.H., Stremler, M.A., Sharp, K.V., Santiago, M.G., Adrian, R.J., Aref, H., Beebe, D.J., "Passive mixing in a three-dimensional serpentine microchannel", *J. Microelectromech. Sys.*, **9** (2), 190—197 (2000).
9 Liu, W.H., Guo, L.J., Wu, T.J., Zheng, X.M., "An experimental study on the flow characteristics of oil-water, two-phase flow in horizontal straight pipes", *Chinese J. Chem. Eng.*, **11** (5), 491 (2003).
10 Bird, R.B., Stewart, W.E., Lightfoot, E.N., Transport Phenomena, John Wiley and Sons, New York, 780—789 (1960).
11 Evensen, H.T., Meldrum, D.R., Cunningham, D.L., "Automated fluid mixing in glass capillaries", *Rev. Sci. Inst.*, **69**, 519—526 (1998).
12 Branebjerg, J., Gravesen, P., Krog, J.P., Nielsen, C.R., "Fast mixing by lamination", In: Pro. IEEEE MEMS Workshop, San Diego, CA, 44—446 (1996).
13 Crampin, E.J., Hackborn, W.W., Maini, P.K., "Pattern formation in reaction-diffusion model with nonuniform domain growth", *Bull Math. Biol.*, **64**, 747—769 (2002).
14 Lide, D.R., Handbook of Chemistry and Physics, 85th ed., CRC Press, London (2004—2005).